

## **SAFETY ASSESSMENT OF EXISTING PILED FOUNDATIONS IN LIQUEFIABLE SOILS AGAINST BUCKLING INSTABILITY**

Subhamoy Bhattacharya

Department of Engineering Science and Somerville College  
University of Oxford, OX1 3PJ, U.K.

### **ABSTRACT**

Collapse of pile-supported structures in liquefiable deposits is still observed after strong earthquakes despite the fact that large factors of safety (against bending due to lateral loads and axial capacity) are employed in their design. Currently, piles in liquefiable soils are designed as beams to avoid bending failure arising from lateral inertial and kinematic (lateral spreading) loads. Recent research suggests that part of the pile in liquefiable soils needs to be treated as unsupported structural columns to avoid buckling instability. Essentially, piles should be treated as columns carrying lateral loads. Beam bending and column buckling require different approaches in design. Designing against bending would not automatically suffice for the buckling requirements. To avoid buckling instability, there is a requirement of minimum diameter of the pile depending on the depth to which the pile may be unsupported owing to liquefaction. In addition, there is also a need to reconsider the safety of the existing piled foundations designed based on the bending mechanism. This paper discusses a method to identify the existing pile-supported structures that are vulnerable to buckling instability.

**KEYWORDS:** Buckling, Bending, Pile, Collapse, Liquefaction

### **INTRODUCTION**

#### **1. Bending and Buckling Instability of Piles during Earthquake Liquefaction**

Collapse of pile-supported structures is still observed in liquefiable soils after strong earthquakes; see for example the building collapses in Figures 1(a) and 1(b). In both cases the buildings had to be demolished following the earthquake. The overall failure pattern for these buildings may appear to be the same in the sense that both of them severely tilted, but they were founded on different types of grounds. The building in Figure 1(a) was located in a laterally spreading ground where the quay wall near the building laterally displaced by more than a metre. On the other hand, the building in Figure 1(b) was located in a level ground at the centre of Fukaehama, Higashinada-Ku, Japan. This building settled by about 1.1 m and also tilted considerably. Permanent ground displacement was not observed in the vicinity of the site.

The current understanding of the failure of the foundations as observed in Figure 1 is as follows. Soil liquefies, losing its shear strength, causing it to flow taking with it any overlying non-liquefied crust. These soil layers drag the pile with them, causing a bending failure. In terms of soil-pile interaction, this mechanism assumes that the soil pushes the pile (Hamada and O'Rourke, 1992; Finn and Fujita, 2002). Figure 2 schematically describes this failure mechanism. Unanimity among various researchers led the Japanese Code of Practice JRA (JRA, 1996) to introduce this concept in the highway design practice (see Figure 3). JRA (1996) recommends practicing engineers to design against bending failure assuming that the non-liquefied crust exerts passive earth pressure on the pile and that the liquefied soil offers 30% of the total overburden pressure. It is also mentioned in the code to check separately against bending failure due to inertial loads and not to add the effects of lateral spreading and inertia. The background of such a clause is described in Ishihara (1997). Other codes, such as Eurocode 8, Part 5 (CEN, 2004), BSSC (2000), also focus on the bending strength of the pile. Hamada (2000) concluded that permanent displacement of non-liquefied crust overlying the liquefied soil is a governing factor for pile damage. A similar conclusion was also reached by Berrill et al. (2001), while analyzing the Landing Bridge performance during the 1987 Edgecumbe earthquake at New Zealand.

However, a recent investigation has demonstrated that fully embedded end-bearing piles passing through loose to medium dense sand may become laterally unstable under the axial load alone as the soil

surrounding the pile liquefies during an earthquake (see Bhattacharya et al., 2004; Knappett and Madabhushi, 2006). The stress in the pile section will be initially elastic and the buckling length will be the entire length of the pile in the liquefied soil. Lateral loading due to slope movement, inertia or out-of-straightness will increase the lateral deflections, which in turn will induce plasticity in the pile and reduce the buckling load, thus promoting a more rapid collapse. These lateral loads are, however, secondary to the basic requirement that piles in liquefiable soil must be checked against Euler's buckling. In other words, part of the pile in liquefiable soil needs to be treated as an unsupported structural column. Crucially, a pile must not be close to buckling when the surrounding soil liquefies.



(a)



(b)

Fig. 1 (a) Collapse of a pile-supported building during the Kobe earthquake; (b) Failure of a piled foundation in level ground during the 1995 Kobe earthquake (courtesy: K. Tokimatsu)

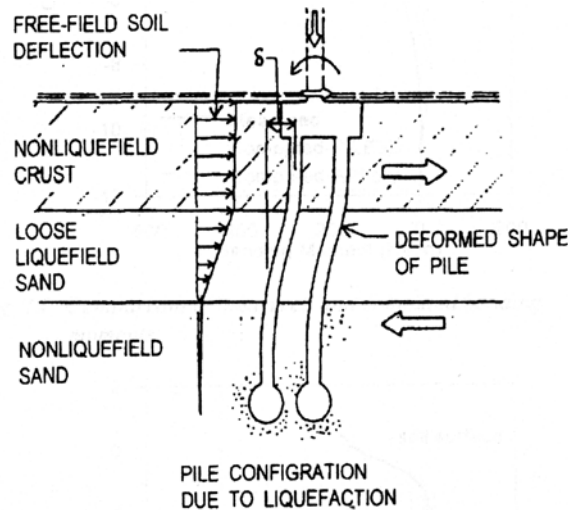


Fig. 2 Pile failure as per the current understanding (after Finn and Thavaraj, 2001)

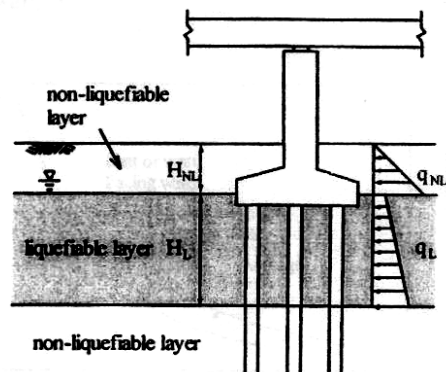


Fig. 3 Idealization of the pile design as in JRA (1996) ( $q_{NL}$  denotes passive earth pressure and  $q_L$  denotes 30% of overburden pressure)

## 2. Purpose of This Paper

In structural design, column buckling and beam bending are approached in different ways. Designing against bending would not necessarily suffice for the requirements to avoid buckling. In this context, it is necessary to highlight the recent interpretation of the failure of piles of the Showa Bridge. Bhattacharya et al. (2005) have shown that while the design of the piles of the bridge satisfied the bending calculations of the recent Japanese codes, e.g., JRA (1996), with a factor of safety of 1.84, the bridge collapsed during the 1964 Niigata earthquake. It has been shown that the piles were unsafe against buckling instability. It has been also argued in this paper that the bridge might have collapsed due to instability of the piles following earthquake-induced liquefaction.

Bending is a stable mechanism as long as the pile is elastic, i.e., if the lateral load is withdrawn, the pile comes back to its initial configuration. This failure mode depends on the bending strength (moment for first yield,  $M_Y$ , or plastic moment capacity  $M_P$ ) of the member under consideration. On the other hand, buckling is an unstable mechanism. It is sudden and occurs when the elastic critical load is reached. It is the most destructive mode of failure and depends on the geometrical properties of the member, i.e., slenderness ratio, and not on the yield strength of the material. Bending failure may be avoided by increasing the yield strength of the material, i.e., by using high-grade concrete or additional reinforcement, but this may not suffice to avoid buckling. To avoid buckling, there should be a minimum pile diameter depending on the depth of the liquefiable soil. There is thus a need to reconsider the safety of the existing piled foundations, designed by using current codes of practice and thus based on the bending mechanism. This paper aims to propose a simplified method to evaluate the safety of the existing piled foundations against the buckling mechanism.

**A SIMPLIFIED METHOD TO IDENTIFY THE EXISTING UNSAFE STRUCTURES AGAINST BUCKLING**

The case of a piled building similar to those in Figure 1 is considered to demonstrate the methodology. This section explains the background of such a methodology. It has been observed through the analysis of pore pressure data in centrifuge tests (Bhattacharya et al., 2005) that as shaking starts, the pore pressure rises such that the condition of zero effective stress is achieved first at the top surface of soil, advancing swiftly downwards as a liquefaction front. It has been hypothesised that, with the advancement of this front, the pile will progressively lose the lateral bracing of the surrounding grains. When this advancing front reaches a “critical depth ( $H_C$ )”, the piled structure will become unstable and will sway in the direction of least lateral stiffness, shearing the initially liquefied soil and eventually rupturing the pile. Therefore, the parameter “critical depth ( $H_C$ )” is the unsupported length of the pile required for buckling instability. A piled structure will become unstable when the “critical depth ( $H_C$ )” becomes less than the unsupported length ( $D_L$ ), provided that the earthquake intensity is strong enough to cause liquefaction to this depth. Clearly,  $D_L$  represents the depth to which the soil is likely to liquefy (loss of soil stiffness) and is, therefore, a function of ground conditions and the expected earthquake at the site. Figure 4 explains the situation by considering an example.

The scenario presented in Figure 4 would represent a bridge pier or a pile-supported structure in the ports and harbours where the water table is at the surface. However, in many cases there will be a substantial crust of stabilised soil or unsaturated sand, which may modify the top boundary conditions of the pile when checking against buckling. If that stiff soil layer is present as a non-liquefied crust at the top of the pile, it remains to be asked whether the crust is free to translate or not. If the crusts spread laterally, as in Figure 2, it must follow that no restraint can be offered against sway of the pile crest, and this will become similar to the case described in Figure 4.

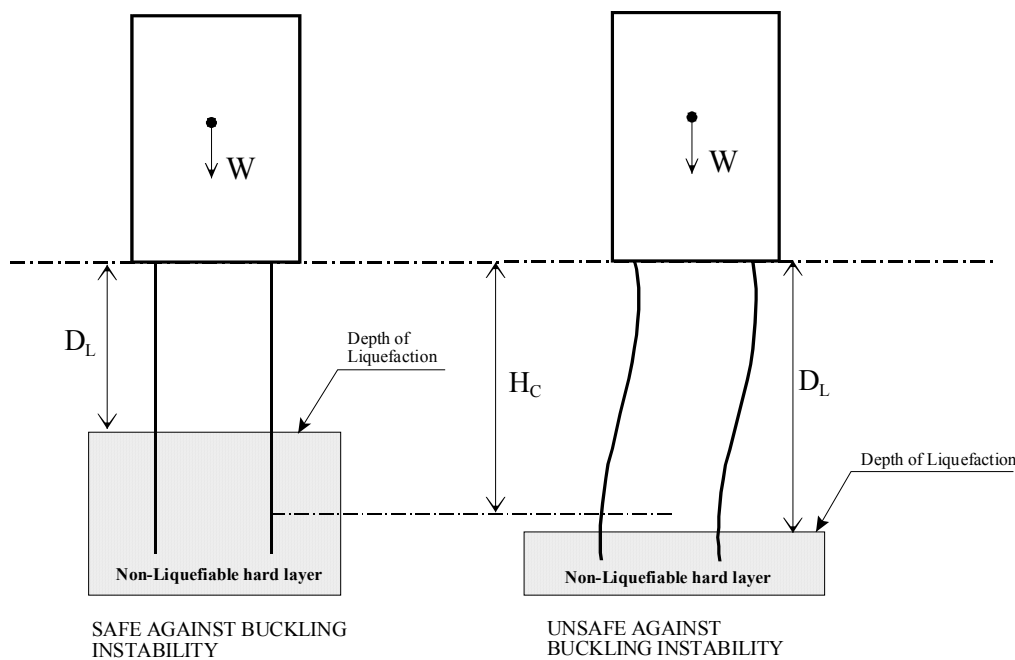


Fig. 4 Schematic diagram showing the concept of “critical depth” and “depth of liquefaction”

**MATHEMATICAL FORMULATION**

**1. Axial Load Acting at Failure**

This section of the paper describes the mathematical background of the proposed methodology.  $P_{static}$  is the static axial load acting on each pile beneath the building assuming that each pile is equally loaded

during the static condition neglecting any eccentricity of loading. However during earthquakes, inertial action of the superstructure will impose dynamic axial loads on the piles, which will increase the total axial load on some piles. This increase may range from 10% to as high as 50% depending on various factors such as the type of superstructure, height of the centre of mass of the superstructure, frequency and magnitude of the earthquake ground motion. This factor is termed as “dynamic axial load factor” denoted by  $\alpha$ . Equation (1) gives an estimate of the maximum axial load acting on a pile.

$$P_{\text{dynamic}} = (1 + \alpha)P_{\text{static}} \quad (1)$$

## 2. Buckling Load of the Pile

For buckling analysis, each pile needs to be evaluated with respect to its end conditions, i.e., fixed, pinned or free. Each pile in a group of identical piles will have the same buckling load as a single pile. If a group of piles is fixed in a stiff pile cap and embedded sufficiently at the tip, as shown in Figure 4, the pile group will buckle in side-sway. The “elastic critical load” of a single pile,  $P_{cr}$ , can be estimated as

$$P_{cr} = \frac{\pi^2 EI}{L_{\text{eff}}^2} \quad (2)$$

where  $L_{\text{eff}}$  is the Euler’s buckling length of a strut pinned at both ends and  $EI$  is the bending stiffness of the pile. Further details on the effective length of the pile can be found in Bhattacharya et al. (2004, 2005).

The piles in this paper will be assumed to have an effective length ( $L_{\text{eff}}$ ) equal to the unsupported length ( $D_L$ ). The unsupported length of the pile is equal to the thickness of liquefiable soil plus some additional length necessary for fixity at the bottom of the liquefiable soil. Typical calculations show that this depth for fixity is about 3 to 5 times the diameter of the pile.

## 3. Failure Load of the Pile

Experiments show that the actual failure load of slender columns is much lower than that predicted by Equation (2). Rankine (1866) recognized that the actual failure involves an interaction between the elastic and plastic modes of failure. Lateral loads or inevitable geometrical imperfections lead to bending moments in addition to the axial loads. These bending moments are accompanied by stress resultants that diminish the cross-sectional area available for carrying the axial load, and therefore the failure loads  $P_{\text{Failure}} < P_{cr}$ . Equally, the growth of zones of plastic bending reduces the effective elastic modulus of the section, thereby reducing the critical load for buckling. Furthermore, these processes feed each other as explained in Horne and Merchant (1965). As the elastic critical load is approached, all bending effects are magnified. Stability analysis of elastic columns (Timoshenko and Gere, 1961) shows that if lateral loads in the absence of axial load create a maximum lateral displacement  $\delta_0$  in the critical mode-shape of buckling, then the displacement  $\delta$  under the same lateral loads but with co-existing axial load  $P$  is given by

$$\frac{\delta}{\delta_0} = \frac{1}{\left(1 - \frac{P}{P_{cr}}\right)} \quad (3)$$

The term  $\delta/\delta_0$  can be termed as the “buckling amplification factor”. It is a measure of the amplification of lateral displacements due to the presence of axial load. Figure 5 presents a graph of this factor plotted against the normalized axial load ( $P/P_{cr}$ ). It can be observed from the graph and Equation (3) that if the applied load is 50% of  $P_{cr}$ , the amplification of lateral deflection due to lateral loads is about two times. At these large deflections, secondary moments will be generated that will lead to more deflections and thus to more  $P-\Delta$  moments. It would, therefore, be important in Figure 5 to be in the linear regime and not in anyway near the asymptotic region. It would also be unwise to use a factor of safety less than 3 against the Euler load of a pile, and therefore,  $P/P_{cr} < 0.33$ . In this case, there is little chance of amplification of the lateral deflections due to axial loads as the point would lie in the linear range of

Figure 5. Structural engineers generally prefer to provide a factor of safety of at least 3 against linear elastic buckling to take into account the eccentricity of load, deterioration of elastic stiffness due to plastic yielding, and unavoidable imperfections. The actual failure load ( $P_{failure}$ ) is therefore some factor,  $\psi$  ( $\psi < 1$ ), times the theoretical Euler’s buckling load and is thus given by

$$P_{failure} = \psi P_{cr} \tag{4}$$

Based on the above discussion, instability may be expected at the axial loads around  $0.35 P_{cr}$ , and therefore,  $\psi$  is taken as 0.35. However, this factor will actually depend on the axial load ( $P_{dynamic}$ ), imperfections, and the residual stresses in the pile due to driving.

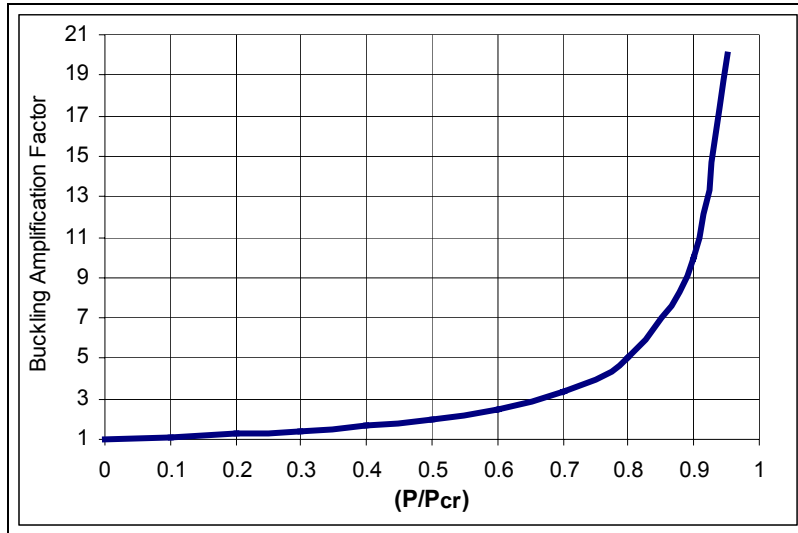


Fig. 5 Buckling amplification factor plotted against the normalized axial load

**4. Determination of “Critical Depth”  $H_C$**

In the limiting condition of failure,  $P_{dynamic} = P_{failure}$ . For the type of structure shown in Figure 4,  $L_{eff} = H_C$ , and thus the limiting axial load that can be applied is obtained from Equations (2) and (4) as

$$P_{dynamic} = 0.35P_{cr} = \frac{0.35\pi^2 EI}{H_C^2} \tag{5}$$

Rearranging this equation gives the estimate of “critical depth”  $H_C$  for a pile shown in Figure 4 as

$$H_C = \sqrt{\frac{3.45EI}{P_{dynamic}}} \tag{6}$$

**5. Limit State Function for Stability**

The stability of a piled foundation under the action of axial load is a function of the depth of liquefaction ( $D_L$ ) and the “critical depth” ( $H_C$ ). Mathematically, the failure surface equation, which defines the stability, is expressed as

$$g(\mathbf{X}) \equiv H_c - D_L \tag{7}$$

where

$H_C$  = critical pile depth calculated from Equation (6) or similar formula based on the boundary conditions of the pile at the top and bottom of the liquefied soil;

$D_L$  = unsupported length = depth of liquefaction + fixity depth at the dense hard layer below the liquefiable layer; depth of liquefaction can be estimated using standard methods; and  
 $\mathbf{X}$  = vector representing the set of variables that will govern the stability of a particular piled foundation at a site for a design earthquake.

The variables in  $\mathbf{X}$  can be classified into four categories as follows:

- (a) Earthquake Characteristics: The random variables identified are  $M$  (moment magnitude) and PGA (Peak Ground Acceleration).
- (b) Pile Characteristics: The pile characteristics can be  $P_{dynamic}$ , Young's Modulus  $E$  of the material of the pile, and pile diameter.
- (c) Soil Profile and Ground Condition: The soil at the site can be characterized by the SPT profile and the average fines content (FC) over the entire profile. The location of water table is also a variable as it determines the depth of liquefaction.
- (d) Type of Superstructure: The superstructure will dictate the "dynamic axial load factor"  $\alpha$  defined by Equation (1) and "buckling amplification factor due to lateral load"  $\psi$  defined in Equation (4).

In Equation (7),  $g(\mathbf{X}) < 0$  indicates failure state;  $g(\mathbf{X}) = 0$  indicates limit state; and  $g(\mathbf{X}) > 0$  indicates safe state. Failure in this context would mean that a piled foundation would become laterally unstable under the axial load and inevitable imperfections when the soil surrounding the piles liquefies.

**A CASE STUDY**

This section of the paper considers the piled foundation in Figure 1(a) to demonstrate the application of the methodology illustrated in the previous section. The building was located 6 m from the quay wall on a reclaimed land in the Higashinada-ku area of Kobe city. Following the 1995 Kobe earthquake, the quay wall got displaced by 2 m towards the sea and the building tilted by 3 degrees. Figure 6 shows the post-earthquake failure investigation of the building. Table 1 summarizes the design data of the building. The building was constructed in early 1980's and was supported on 38 hollow, prestressed concrete piles (see Figure 7). Table 2 summarizes the design data of the pile. The arrangement of the piles in the foundation is shown in Figure 8. From the foundation plan, it is clear that the structure is moment-resisting RCC frame with tie beams at the foundation level. Figure 9 shows the boring log of the site at two locations. Input motion measured at the nearby Higashi-Kobe bridge showed a peak ground acceleration of 0.38g. However, the PGA at the building site is not known. Extensive soil liquefaction and sand boils were observed in the area. The static axial load ( $P_{static}$ ) acting under the building is reported to be 412 kN (Uzuoka et al., 2002).

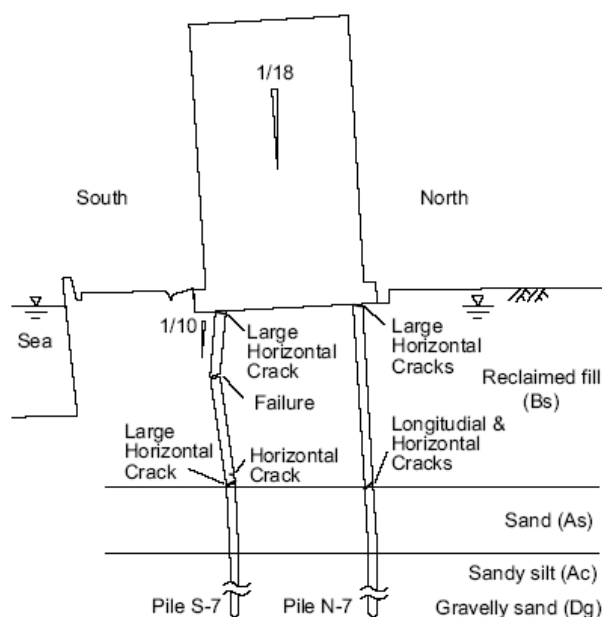


Fig. 6 Post-earthquake investigation of the building

**Table 1: Design Data of the Building**

<b>Building Height</b>	14.5 m above Ground Level
<b>Building Dimensions</b>	22.675×7 m
<b>Foundation Type</b>	Precast Driven Pile
<b>Building Type</b>	R.C.C. Framed
<b>Number of Stories</b>	5
<b>Axial Load on Each Pile</b>	412 kN
<b>Dead Load of the Building</b>	15656 kN

**Table 2: Design Data of Pile**

<b>Length</b>	20 m
<b>External Diameter</b>	400 mm
<b>Internal Diameter</b>	240 mm
<b>Material</b>	Prestressed Concrete
<b>Young's Modulus <math>E</math></b>	30 GPa
<b><math>EI</math></b>	32.35 MN-m <sup>2</sup>



Fig. 7 Piles used in the building

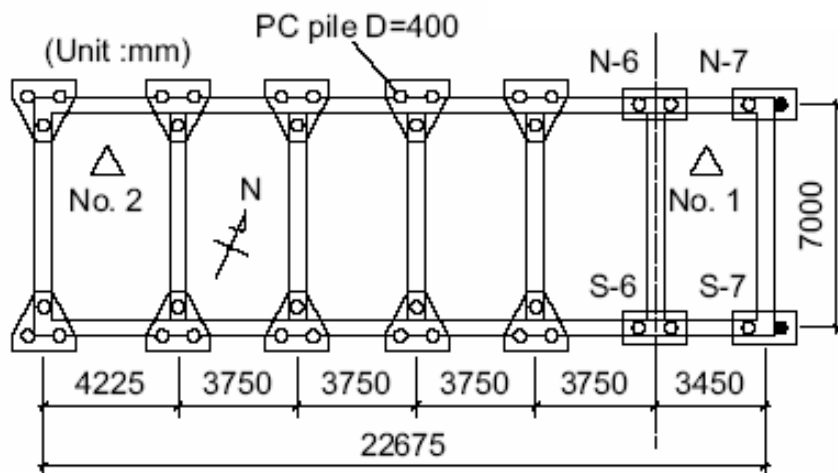


Fig. 8 Foundation plan showing the piles



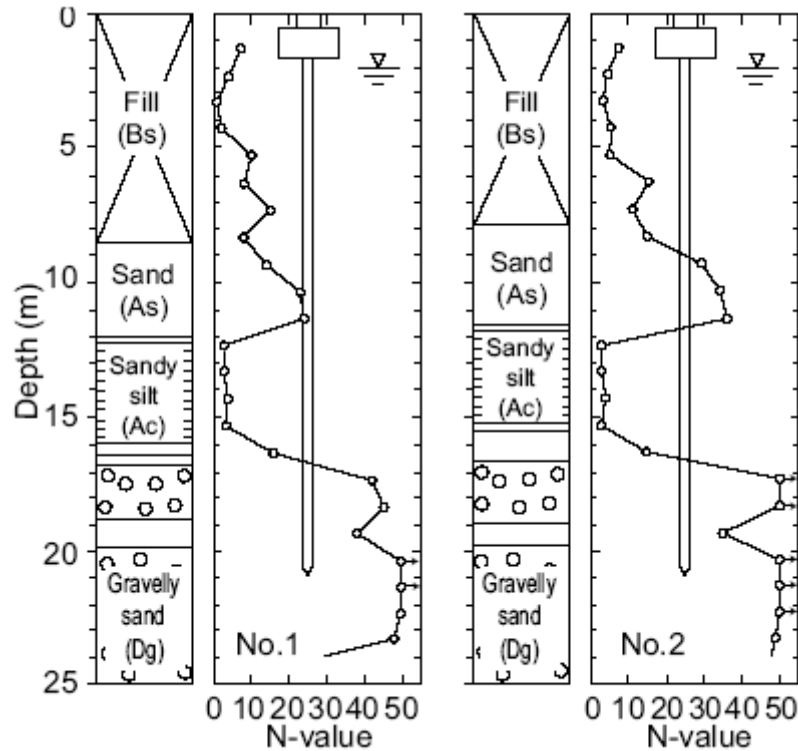


Fig. 9 Boring log of the soil at two locations at the site

**1. Liquefaction and Site Response Analysis**

The water table at the site was located 2 m below the ground level. It has been reported that 10 m of soil liquefied and therefore, the depth of liquefaction was 12 m. The boring log also suggests that the soil below the liquefied layer between 12 and 15 m consists of sandy silt (Ac) and has very low strength. This layer is composed of a clayey soil and it is most likely that it did not liquefy. However, the SPT value is less than 3 and no fixity against the lateral load could be expected from this layer. It can therefore be inferred that the plane of fixity of the pile against lateral loads after full liquefaction was few pile diameters below 15 m.

**2. Effect of the Non-liquefied Crust in the Sway Mode of Unstable Collapse**

Where piles of diameter  $D$  pass through a depth more than  $5D$  of stiff non-liquefiable soil, it would not be unreasonable to take that portion of the pile as restrained against rotation. If the portion passing through  $5D$  of stiff soil is at the pile toe, and there is no lower layer of liquefied material, the toe also could be regarded as being fixed in location. In addition to the fixity at the pile toe, if the non-liquefied crust above the liquefiable soil was somehow prevented from sliding, as in the rather unlikely scenario in the case of earthquakes, the pile could at best be regarded as completely fixed at both ends. In such a case,  $L_{eff}$  (effective length) of the pile would be equal to half of the unsupported length of the pile (liquefiable soil thickness + depth required for fixity). In the building under consideration, even though the pile passes through  $5D$  in the crust, the non-liquefied crusts might have spread laterally. It must, therefore, follow that no restraint could be offered against sway of the pile crest, and the boundary conditions would be similar to the case described in Figure 4.

Various steps in the safety analysis are as follows.

**2.1 Estimation of “Dynamic Axial Load Factor” ( $\alpha$ )**

At the onset of the earthquake, as the superstructure starts to oscillate, inertial forces are generated. These inertial forces are transferred as lateral forces and overturning moments to the piles via the pile cap. The pile cap transfers the moments as varying axial loads to the piles. In loose saturated sandy soil, as the shaking continues, pore pressure builds up and the soil starts to liquefy. During and after the liquefaction,

the stiffness of the pile-soil system in the zone of liquefaction reduces and as a result, the period of the structure increases. This section aims to predict the additional axial load acting on the pile during the earthquake shaking for two stages:

(a) *At the onset of the earthquake but before liquefaction*

The seismic base shear acting on the building is usually estimated by the equivalent lateral force procedure as (BSSC, 2000; BIS, 2002; CEN, 2004)

$$V_B = C_S W \quad (8)$$

where  $W$  denotes total weight of the building and  $C_S$  is the seismic response coefficient given as (BIS, 2002)

$$C_S = \frac{ZI_{\text{factor}}}{2R} \left( \frac{S_a}{g} \right) \quad (9)$$

where

$Z$  = zone factor for the Maximum Considered Earthquake;

$I_{\text{factor}}$  = importance factor for the structure;

$R$  = response reduction factor, depending on the perceived seismic damage performance as characterized by the ductile or brittle deformations; and

$S_a / g$  = average response acceleration coefficient, which is a function of the building site and the period of the structure.

Traditionally, the fundamental vibration period of R.C.C buildings is estimated by using internationally calibrated data. The approximate fundamental natural period of vibration ( $T_a$ ), in seconds, of a moment-resisting frame building with brick infill panels may be estimated as (BIS, 2002)

$$T_a = \frac{0.09h}{\sqrt{d}} \quad (10)$$

where  $h$  denotes the height of the building in m (for the building under consideration, the height is 14.5 m), and  $d$  is the base dimension of the building at the plinth level, in m, along the direction of the lateral force. This dimension is 7 m for the building under consideration.

The period based on Equation (10) has been calculated to be 0.49 s. The soil in the building site can be classified as soft soil based on IS 1893 (Part 1)-2002 (BIS, 2002), and therefore, the spectral acceleration for different periods can be calculated from

$$\frac{S_a}{g} = \begin{cases} 1 + 15T_a & ; \quad 0.0 \leq T_a \leq 0.10 \\ 2.5 & ; \quad 0.10 \leq T_a \leq 0.67 \\ 1.67 / T_a & ; \quad 0.67 \leq T_a \leq 4.0 \end{cases} \quad (11)$$

where  $T_a$  denotes period of the building.

It has been reported that the seismic coefficient  $C_S$  for the example case was 0.4 (Tokimatsu and Asaka, 1998). Therefore, the base shear of the building can be estimated as

$$V_B = 0.4 \times 15656 = 6264 \text{ kN} \quad (12)$$

This base shear would be resisted by the foundation piles. The lateral load on each pile was therefore 165 kN. Davisson and Robinson (1965) developed an approximate method to analyze laterally loaded piles. In this procedure, a laterally loaded pile is assumed to be fixed at some point in the ground, the depth of which depends on the relative stiffness between the soil and the pile. This method, widely used in practice, involves the computation of stiffness factor  $T$  for a particular combination of pile and soil as

$$T = \sqrt[5]{\frac{EI}{\eta_h}} \quad (13)$$

where  $EI$  denotes stiffness of the pile and  $\eta_h$  is the modulus of subgrade reaction having units of force/(length)<sup>3</sup>. Typical values of  $\eta_h$  are shown in Table 3.

**Table 3: Values of the Modulus of Subgrade Reaction**

Relative Density	Value of $\eta_h$ (MN/m <sup>3</sup> )	
	Sand below the Water Table	Sand above the Water Table
40%	8	13
60%	24	42
80%	40	75

The depth-to-pile-diameter ratio to the point of fixity is taken as  $1.8T$  for granular soils whose modulus increases linearly with depth. The point of fixity in the present case is obtained as follows.

The average SPT-N value at the top layer is 3, and therefore the relative density can be estimated by following equation. This empirical correlation between SPT-N, effective vertical stress and % relative density (RD) was proposed by Meyerhof (1957).

$$RD = 21 \sqrt{\frac{N}{\sigma'_v + 0.7}} \tag{14}$$

Here  $N$  denotes the SPT–N value and  $\sigma'_v$  the vertical effective stress in kgf/cm<sup>2</sup>.

For the SPT-N value of 3, the relative density is estimated to be about 40% and therefore the modulus of subgrade reaction becomes 8 MN/m<sup>3</sup>. The stiffness factor  $T$ , defined by Equation (13), can be calculated as

$$T = \sqrt[5]{\frac{32.35}{8}} = 1.32 \text{ m} \tag{15}$$

Thus, the point of fixity is at 2.4 m depth. Figure 10 explains this situation. The rocking moment in the foundation can be estimated as

$$M_R = 6264 \times 2.4 = 15033 \text{ kN-m} \tag{16}$$

The additional axial compressive load acting on each pile is given by following equation:

$$P_{inc} = \frac{15033}{7 \times 19} = 113 \text{ kN} \tag{17}$$

It may be mentioned that 19 piles are sharing the additional axial load on one side. This calculation shows that the increase in axial load is about 27%.

*(b) Just after liquefaction*

As mentioned earlier, at full liquefaction the base shear due to earthquake excitation will be reduced. To estimate the reduced base shear, it is necessary to predict the period of vibration of the building for small vibrations when the soil surrounding the pile has liquefied. Considering the fixity at about 2 m below the soft zone, it follows that the pile will be fixed at about 17 m below the ground level. The stiffness of the building for small vibrations at full liquefaction is given by following equation:

$$k = 38 \times \frac{12EI}{L^3} = 38 \times \frac{12 \times 32.35}{17^3} = 3 \text{ MN/m} \tag{18}$$

It is assumed here that the stiffness of the piles primarily contributes to the total stiffness of the pile-soil system. This assumption can be justified by the fact that the elastic stiffness of the liquefied soil is orders of magnitude less than that of the concrete pile. The model for estimating stiffness for a single pile is shown in Figure 11. The time period of the building during full liquefaction can thus be estimated as

$$T_{a,Liq} = 2\pi \sqrt{\frac{M}{k}} = 2\pi \sqrt{\frac{15656 \times 1000}{9.8 \times 3 \times 10^6}} = 4.5 \text{ s} \tag{19}$$

where  $M$  is the mass of the building and  $k$  is the stiffness of the building.

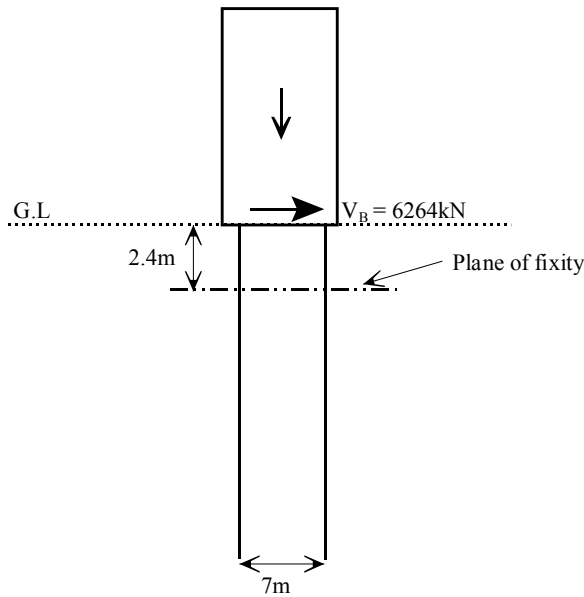


Fig. 10 Fixity of the pile at the onset of earthquake and before liquefaction

The above calculation shows that the time period of vibration would increase by 9 times and, therefore, the base shear in the building would decrease following Equations (9) and (11). It can be immediately inferred that the spectral acceleration would decrease by a factor of 5 and, therefore, the base shear would reduce to 1252 kN. Therefore, the increase in axial load on each pile is given as (see Figure 12)

$$P_{inc} = \frac{1252 \times 17}{7 \times 19} = 160 \text{ kN} \tag{20}$$

This is an increase of about 40%. Though the base shear is reduced by 5 times, it is the lever arm of the moment that has increased by about 7 times. The above calculations show that the axial load might increase by about 40% during the liquefaction stage. Therefore  $\alpha$  can be taken as 0.4.

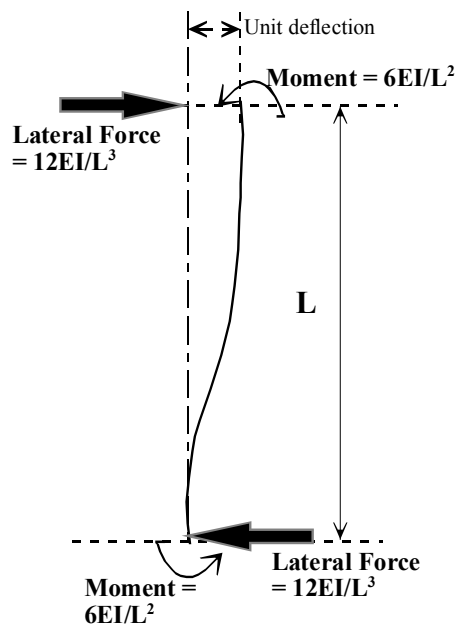


Fig. 11 Stiffness of single pile in the foundation

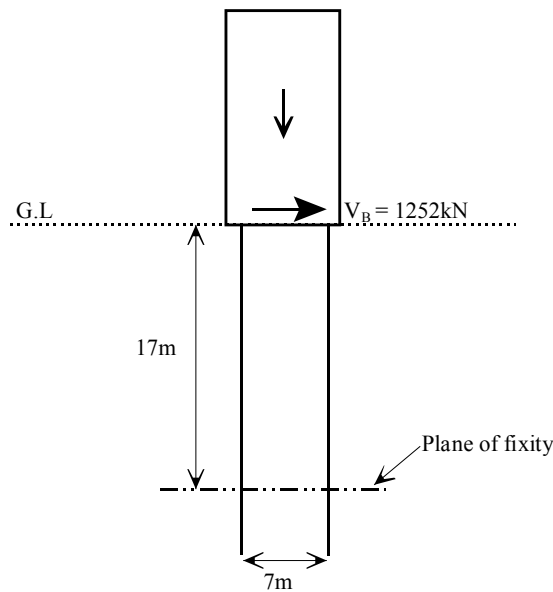


Fig. 12 Fixity of the pile after full liquefaction

**2.2 Estimation of the Critical Depth**

Table 4 shows the details for the estimation of the critical depth.

**Table 4: Estimation of the Critical Depth of the Pile for the Building**

Parameter	Value	Remarks
$P_{static}$	412 kN	Following Uzuoka (2002)
$P_{dynamic}$	$(1 + 0.4) \times 412 = 576$ kN	Following Equation (3); the dynamic axial load factor at full liquefaction is estimated to be 0.4
$H_C$	13.9 m	Following Equation (6)

**2.3 Factor of Safety against Buckling Instability**

The unsupported length ( $D_L$ ) of the pile is about 17 m. As  $D_L > H_C$ , it can be inferred that the building is unsafe against the buckling instability form of failure. The factor of safety against the buckling failure can be estimated by taking the ratio of  $H_C$  and  $D_L$  as

$$\text{Factor of Safety against Buckling} \equiv \frac{H_C}{D_L} = \frac{13.9}{17.0} = 0.81 \tag{21}$$

Mathematically, following Equation (7),  $g(\mathbf{X}) < 0$  that indicates a failure state. The question still remains whether the actual cause of failure for the piles of the building was buckling. The piles being hollow also indicates that those were weak in shear. However, the above calculations have demonstrated that buckling could be one explanation for the cause of failure.

**CONCLUSIONS**

The current methods of pile design are based on a bending mechanism wherein lateral loads due to inertia and slope movement induce bending failure in the pile. Recent research has shown that buckling of piles due to the combined action of axial load and diminishing soil support owing to liquefaction is a feasible pile failure mechanism. Buckling and bending require different approaches in design. Bending is a stable mechanism as long as the pile is elastic, i.e., if the lateral load is withdrawn, the pile comes back to its initial configuration. This failure mode depends on the bending strength (moment for first yield,

$M_Y$ , or plastic moment capacity  $M_p$ ) of the member under consideration. Designing against bending would not automatically suffice for the buckling requirements. There is also a need to re-examine the safety of existing piled foundations designed based solely on bending mechanism.

A simple method to evaluate such safety has been formulated in this paper. This method checks the stability of the foundation against buckling instability at full liquefaction, i.e., when the soil surrounding the pile is at its lowest possible stiffness. Two parameters, namely “critical depth  $H_C$ ” and the “unsupported length of the pile due to liquefaction  $D_L$ ” are estimated. Critical depth is a function of axial load acting on the pile ( $P$ ), flexural stiffness of the pile ( $EI$ ) and the boundary condition of the pile above and below the liquefiable soil. On the other hand,  $D_L$  depends mainly on the earthquake characteristics, soil profile, and the ground conditions. A case study has been considered to illustrate the application of the proposed methodology.

## REFERENCES

1. Berrill, J.B., Christensen, S.A., Keenan, R.P., Okada, W. and Pettinga, J.R. (2001). “Case Studies of Lateral Spreading Forces on a Piled Foundation”, *Géotechnique*, Vol. 51, No. 6, pp. 501-517.
2. Bhattacharya, S., Madabhushi, S.P.G. and Bolton, M.D. (2004). “An Alternative Mechanism of Pile Failure in Liquefiable Deposits during Earthquakes”, *Géotechnique*, Vol. 54, No. 3, pp. 203-213.
3. Bhattacharya, S., Bolton, M.D. and Madabhushi, S.P.G. (2005). “A Reconsideration of the Safety of the Piled Bridge Foundations in Liquefiable Soils”, *Soils and Foundations*, Vol. 45, No. 4, pp. 13-25.
4. BIS (2002). “IS 1893 (Part 1)-2002: Indian Standard Criteria for Earthquake Resistant Design of Structures, Part 1 – General Provisions and Buildings”, Bureau of Indian Standards, New Delhi.
5. BSSC (2000). “The 2000 NEHRP Recommended Provisions for New Buildings and Other Structures, Part 2: Commentary (FEMA 369)”, Building Seismic Safety Council, National Institute of Building Sciences, Washington, DC, U.S.A.
6. CEN (2004). “Eurocode 8: Design of Structures for Earthquake Resistance – Part 5: Foundations, Retaining Structures and Geotechnical Aspects”, EN 1998-5:2004, Comité Européen de Normalisation, Brussels, Belgium.
7. Davisson, M.T. and Robinson, K.E. (1965). “Bending and Buckling of Partially Embedded Piles”, *Proceedings of the Sixth International Conference on Soil Mechanics and Foundation Engineering*, Montreal, Canada, Vol. 2, pp. 243-246.
8. Finn, W.D.L. and Fujita, N. (2002). “Piles in Liquefiable Soils: Seismic Analysis and Design Issues”, *Soil Dynamics and Earthquake Engineering*, Vol. 22, No. 9, pp. 731-742.
9. Finn, W.D.L. and Thavaraj, T. (2001). “Deep Foundations in Liquefiable Soils: Case Histories, Centrifuge Tests and Methods of Analysis”, *Proceedings of the Fourth International Conference on Recent Advances in Geotechnical Engineering and Soil Dynamics*, San Diego, U.S.A., Paper No. SOAP-1 (on CD).
10. Hamada, M. (2000). “Performances of Foundations against Liquefaction-Induced Permanent Ground Displacements”, *Proceedings of the 12th World Conference on Earthquake Engineering*, Auckland, New Zealand, Paper No. 1754 (on CD).
11. Hamada, M. and O'Rourke, T.D. (editors) (1992). “Case Studies of Liquefaction and Lifeline Performance during Past Earthquakes, Volume 1, Japanese Case Studies”, Technical Report NCEER-92-0001, State University of New York at Buffalo, Buffalo, U.S.A.
12. Horne, M.R. and Merchant, W. (1965). “The Stability of Frames”, Pergamon Press, London, U.K.
13. Ishihara, K. (1997). “Geotechnical Aspects of the 1995 Kobe Earthquake”, *Proceedings of the 14th International Conference on Soil Mechanics and Foundation Engineering*, Hamburg, Germany, pp. 2047-2073.
14. JRA (1996). “Design Specifications of Highway Bridges. Part V: Seismic Design”, Japan Road Association, Tokyo, Japan.
15. Knappett, J.A. and Madabhushi, S.P.G. (2006). “Modelling of Liquefaction-Induced Instability in Pile Groups” in “Seismic Performance and Simulation of Pile Foundations in Liquefied and Laterally

- Spreading Ground (edited by R.W. Boulanger and K. Tokimatsu)", Geotechnical Special Publication No. 145, American Society of Civil Engineers, Reston, U.S.A.
16. Meyerhof, G.G. (1957). "Discussion on Research on Determining the Density of Sands by Spoon Penetration Testing", Proceedings of the Fourth International Conference on Soil Mechanics and Foundation Engineering, London, U.K., Vol. 3, p. 110.
  17. Rankine, W.J.M. (1866). "Useful Rules and Tables Relating to Mensuration, Engineering, Structures, and Machines", Charles Griffin and Company, London, U.K.
  18. Timoshenko, S.P. and Gere, J.M. (1961). "Theory of Elastic Stability", McGraw-Hill Book Company, New York, U.S.A.
  19. Tokimatsu, K. and Asaka, Y. (1998). "Effects of Liquefaction-Induced Ground Displacements on Pile Performance in the 1995 Hyogoken-Nambu Earthquake", Soils and Foundations, Special Issue on Geotechnical Aspects of the January 17, 1995 Hyogoken-Nambu Earthquake, No. 2, pp. 163-177.
  20. Uzuoka, R., Sento, N., Yashima, A. and Zhang, F. (2002). "3-Dimensional Effective Stress Analysis of a Damaged Group-Pile Foundation adjacent to a Quay Wall", Journal of JAEE, Vol. 2, No. 2, pp. 1-14.